PHYSICAL REVIEW D **87,** 074027 (2013)

$B_c \to D^{(*)}T$ decays in perturbative QCD approach

Zhi-Tian Zou,[1] Xin Yu,[1] and Cai-Dian Lü[1,2,*]

[1]*Institute of High Energy Physics and Theoretical Physics Center for Science Facilities, Chinese Academy of Sciences, Beijing 100049, People's Republic of China*

[2]*Kavli Institute for Theoretical Physics China, CAS, Beijing 100190, China*

(Received 23 November 2012; published 23 April 2013)

In this work, we investigate $B_c \to D^{(*)}T$ decays in the perturbative QCD approach, based on k_T factorization, where T denotes a light tensor meson. For all decays considered in this work, there are no contributions from factorizable emission diagrams because the emitted tensor meson cannot be generated from (axial-)vector current or (pseudo)scalar density. We find that the annihilation amplitudes are dominant in these decays due to the large Cabibbo-Kobayashi-Maskawa elements, which can be perturbatively calculated without parametrization in the pQCD approach. The branching ratios of the $B_c \to D^{(*)}K_2^*$ decays can reach 10^{-5} to 10^{-4}, which is one order of magnitude larger than that of the corresponding $B_c \to D^{(*)}K^*$ decays, where heavy cancellation occurred between the penguin emission and tree annihilation diagrams. With such large branching ratios, they can very likely be observed in the ongoing LHCb experiments. We also predict a large percentage of transverse polarizations in those W-annihilation-diagram dominant $B_c \to D^*T$ decay channels.

DOI: 10.1103/PhysRevD.87.074027 PACS numbers: 13.25.Hw, 12.38.Bx

I. INTRODUCTION

After the first observation was reported in 1998 by the CDF Collaboration [1], which was confirmed in 2008 by the CDF and D0 Collaborations [2] at the Tevatron in excess of 5σ significance, the study of B_c mesons has become one of the current topics of interest, especially since the Large Hadron Collider (LHC) experiment began running normally. From the point of view, the B_c meson is a ground state of two heavy quarks' system, with a c quark and a $\bar{b}$ quark, which is very different from the symmetric heavy quarkonium ($\bar{c}c, \bar{b}b$) states, due to the flavor $B = -C = \pm 1$ carried by the B_c meson. Since the B_c meson carries explicit flavor, it cannot annihilate via a strong interaction or an electromagnetic interaction like the mesons consisting of $\bar{c}c$ or $\bar{b}b$. It can only decay via a weak interaction. Thus, it provides us with an ideal platform to understand the weak interaction of heavy quark flavor [3,4]. Unlike the heavy-light B_q meson ($q = u, d, s$), both the $\bar{b}$ and c can decay with the other as a spectator, or they can annihilate into pairs of leptons or light mesons. If more data become available, B_c physics might be useful to study the perturbative and nonperturbative QCD dynamics, final state interactions, and even new physics beyond the standard model [3,4]. In recent years, many theoretical studies on the production and decays of the B_c meson have been done based on operator product expansion [5,6], nonrelativistic QCD (NRQCD) and perturbative methods [7–11], QCD sum rules [12,13], $SU(3)$ flavor symmetry [14], the Isgur-Scora-Grinstein-Wise (ISGW) quark model [15–17], the QCD factorization approach [18,19], and the perturbative QCD (PQCD) approach [20–26].

The B meson decays involving a tensor meson have been studied in Refs. [27–40]. In Refs. [16,17], the authors studied some analogous B_c decays involving a tensor meson in final states, but only with the tensor meson as the recoiled meson. In this work, we focus on the $B_c \to D^{(*)}T$ decays, where T denotes a light tensor meson with $J^P = 2^+$. We know that a factorizable amplitude proportional to the matrix element $\langle T \mid j^\mu \mid 0\rangle$, where j^μ is the $(V \pm A)$ or $(S \pm P)$ current, does not contribute because this matrix element vanishes from Lorentz covariance considerations [28,29,33,34]. Thus, these $B_c \to D^{(*)}T$ decays are prohibited in naive factorization. To our knowledge, these decays are never considered in theoretical papers due to this difficulty of factorization. In order to give the predictions to these decay channels, it is necessary to go beyond the naive factorization to calculate the nonfactorizable and annihilation-type diagrams. What is more, the annihilation amplitudes will be dominant in these $B_c \to D^{(*)}T$ decays because they are proportional to the large Cabibbo-Kobayashi-Maskawa (CKM) matrix elements V_{cb} and $V_{cs(d)}$. It is worth mentioning that the annihilation-type diagrams can be perturbatively calculated without parametrization in the PQCD approach [41,42]. The PQCD approach has successfully predicted the pure annihilation-type decays $B_s \to \pi^+\pi^-$ [43,44] and $B^0 \to D_s^- K^+$ [45,46], which have been confirmed by experiments [47,48]. So, for these annihilation dominant decays, the calculation in the PQCD approach is reliable.

In this paper, we shall study these $B_c \to D^{(*)}T$ decays in the PQCD approach, which is based on the k_T factorization [49–51]. In this approach, we keep the transverse momentum of quarks, and as a result, the end-point singularity in collinear factorization can be avoided. On the other hand, the double logarithms will appear in the QCD correction

*lucd@ihep.ac.cn

due to the additional energy scale introduced by the transverse momentum. Using the renormalization group equation, the double logarithms can be resummed, which results in the Sudakov form factor. This factor effectively suppresses the end-point contribution of the distribution amplitude of mesons in the small transverse momentum region, which makes the calculation in the PQCD approach reliable and consistent.

In these decays, there is one more intermediate energy scale, the c quark mass. As a result, another expansion series of m_c/m_{B_c} will appear. So far, the factorization has been approved at the leading order of m_c/m_{B_c} expansion [52,53], which has also been proved by soft collinear effective theory [54]. We consider only the leading order contribution of the expansion for each kind of diagram, not the same order for all the diagrams. The factorization should be improved in this power expansion order by order.

This paper is organized as follows. In Sec. II, we present the formalism and wave functions of the considered decays. Then, we perform the perturbative calculations for the considered decay channels with the PQCD approach in Sec. III. The numerical results and phenomenological analysis are given in Sec. IV. Finally, Sec. V contains a short summary.

II. FORMALISM AND WAVE FUNCTION

In order to give the predictions for these considered $B_c \to D^{(*)}T$ decays, the key step is to calculate the transition matrix elements:

$$\mathcal{M} \propto \langle D^{(*)}T|\mathcal{H}_{\text{eff}}|B_c\rangle, \tag{1}$$

where the weak effective Hamiltonian $\mathcal{H}_{\text{eff}}$ can be written as [55]

$$\mathcal{H}_{\text{eff}} = \frac{G_F}{\sqrt{2}}\Bigg\{\sum_{q=u,c} V_{qb}^* V_{qX}[C_1(\mu)O_1^q(\mu) + C_2(\mu)O_2^q(\mu)] - V_{tb}^* V_{tX}\Bigg[\sum_{i=3}^{10} C_i(\mu)O_i(\mu)\Bigg]\Bigg\}, \tag{2}$$

with $V_{qb(X)}$ and $V_{tb(X)}$ ($X = d, s$) the CKM matrix elements. $O_j (j = 1, \ldots, 10)$ are the local four-quark operators:

current-current (tree) operators

$$\begin{aligned} O_1^q &= (\bar{b}_\alpha q_\beta)_{V-A}(\bar{q}_\beta X_\alpha)_{V-A}, \\ O_2^q &= (\bar{b}_\alpha q_\alpha)_{V-A}(\bar{q}_\beta X_\beta)_{V-A}, \end{aligned} \tag{3}$$

QCD penguin operators,

$$\begin{aligned} O_3 &= (\bar{b}_\alpha X_\alpha)_{V-A}\sum_{q'}(\bar{q}'_\beta q'_\beta)_{V-A}, \\ O_4 &= (\bar{b}_\alpha X_\beta)_{V-A}\sum_{q'}(\bar{q}'_\beta q'_\alpha)_{V-A}, \end{aligned} \tag{4}$$

$$\begin{aligned} O_5 &= (\bar{b}_\alpha X_\alpha)_{V-A}\sum_{q'}(\bar{q}'_\beta q'_\beta)_{V+A}, \\ O_6 &= (\bar{b}_\alpha X_\beta)_{V-A}\sum_{q'}(\bar{q}'_\beta q'_\alpha)_{V+A}, \end{aligned} \tag{5}$$

and electroweak penguin operators,

$$\begin{aligned} O_7 &= \frac{3}{2}(\bar{b}_\alpha X_\alpha)_{V-A}\sum_{q'}e_{q'}(\bar{q}'_\beta q'_\beta)_{V+A}, \\ O_8 &= \frac{3}{2}(\bar{b}_\alpha X_\beta)_{V-A}\sum_{q'}e_{q'}(\bar{q}'_\beta q'_\alpha)_{V+A}, \end{aligned} \tag{6}$$

$$\begin{aligned} O_9 &= \frac{3}{2}(\bar{b}_\alpha X_\alpha)_{V-A}\sum_{q'}e_{q'}(\bar{q}'_\beta q'_\beta)_{V-A}, \\ O_{10} &= \frac{3}{2}(\bar{b}_\alpha X_\beta)_{V-A}\sum_{q'}e_{q'}(\bar{q}'_\beta q'_\alpha)_{V-A}, \end{aligned} \tag{7}$$

where α and β are the color indices and q' are the active quarks at the scale m_b, i.e., $q' = (u, d, s, c, b)$. The left-handed and right-handed currents are defined as $(\bar{b}_\alpha q_\beta)_{V-A} = \bar{b}_\alpha \gamma_\mu (1-\gamma_5) q_\beta$ and $(\bar{q}'_\beta q'_\alpha)_{V+A} = \bar{q}'_\beta \gamma_\mu (1+\gamma_5) q'_\alpha$, respectively. The combinations a_i of the Wilson coefficients are defined as [56]

$$\begin{aligned} a_1 &= C_2 + C_1/3, \qquad a_2 = C_1 + C_2/3, \\ a_i &= C_i + C_{i+1}/3, \qquad i = 3, 5, 7, 9, \\ a_j &= C_j + C_{j-1}/3, \qquad j = 4, 6, 8, 10. \end{aligned} \tag{8}$$

In hadronic B decays, there are several typical scales, and expansions with respect to the ratios of the scales are usually carried out. The electroweak physics higher than the W boson mass can be calculated perturbatively. The physics between the b quark mass scale and the W boson mass scale can be included in the Wilson coefficients $C_i(\mu)$ of the effective four-quark operators, which are obtained by using the renormalization group equation. The physics between M_B and the factorization scale is included in the calculated hard part in the PQCD approach. The physics below the factorization scale is nonperturbative and described by the hadronic wave functions of mesons, which are universal for all decay modes. Finally, in the PQCD approach, the decay amplitude can be factorized into the convolution of the Wilson coefficients $C(t)$, the hard scattering kernel, and the light-cone wave functions $\Phi_{M_i,(B)}$ of mesons characterized by different scales,

$$\mathcal{A} \sim \int dx_1 dx_2 dx_3 b_1 db_1 b_2 db_2 b_3 db_3 \times \text{Tr}[C(t)\Phi_B(x_1, b_1) \times \Phi_{M_2}(x_2, b_2)\Phi_{M_3}(x_3, b_3)H(x_i, b_i, t)S_t(x_i)e^{-S(t)}], \tag{9}$$

where b_i is the conjugate variable of the quark transverse momentum k_{iT}, x_i is the momentum fraction of valence quarks, and t is the largest scale in the hard part $H(x_i, b_i, t)$.

The jet function $S_t(x_i)$, which is obtained by the threshold resummation, smears the end-point singularities on x_i [57]. The Sudakov form factor $e^{-S(t)}$ is from the resummation of the double logarithms, which suppresses the soft dynamics effectively, i.e., the long-distance contributions in the large b region [58,59]. Thus, it makes the perturbative calculation of the hard part H applicable at intermediate scales, i.e., the m_B scale.

In the PQCD approach, the initial and final state meson wave functions are the most important nonperturbative inputs. For the B_c meson, we only consider the contribution from the first Lorentz structure, like the $B_q(q = u, d, s)$ meson,

$$\Phi_{B_c}(x) = \frac{i}{\sqrt{2N_c}}(\not{P} + m_{B_c})\gamma_5 \phi_{B_c}(x, b). \tag{10}$$

For the distribution amplitude, we adopt the model [20]

$$\phi_{B_c}(x,b) = \frac{f_{B_c}}{2\sqrt{2N_c}}\delta(x - m_c/m_{B_c})\exp\left[-\frac{1}{2}w_{B_c}^2 b^2\right], \tag{11}$$

in which $\exp[-\frac{1}{2}w_{B_c}^2 b^2]$ represents the k_T dependence. f_{B_c} and $N_c = 3$ are the decay constant of the B_c meson and the color number, respectively. So far, there are not enough experimental data to constrain the wave function and the distribution amplitude of the B_c meson. On the other hand, because the c quark is massive (relative to the known light quarks u, d, and s), we approximatively take the leading order wave function without the spread. In fact, a spread of the c quark momentum acts the same as the change of its central value. Fortunately, for these considered decays, the dominant contributions are from the annihilation-type diagrams, which do not depend heavily on the shape of the B_c meson distribution amplitude.

As discussed in Ref. [27], for these $B_c \to D^{(*)}T$ decays, the ± 2 polarizations ($J^P = 2^+$) do not contribute due to the angular momentum conservation argument. Because of the simplification, the wave functions for a generic tensor meson are defined by [27]

$$\Phi_T^L = \frac{1}{\sqrt{6}}\left[m_T \not{\epsilon}^*_{\bullet L}\phi_T(x) + \not{\epsilon}^*_{\bullet L}\not{P}\phi_T^t(x) + m_T^2 \frac{\epsilon_\bullet \cdot v}{P \cdot v}\phi_T^s(x)\right]$$
$$\Phi_T^\perp = \frac{1}{\sqrt{6}}[m_T \not{\epsilon}^*_{\bullet \perp}\phi_T^v(x) + \not{\epsilon}^*_{\bullet \perp}\not{P}\phi_T^T(x) + m_T i\epsilon_{\mu\nu\rho\sigma}\gamma_5\gamma^\mu \epsilon^{*\nu}_{\bullet \perp} n^\rho v^\sigma \phi_T^a(x)], \tag{12}$$

where $\epsilon_\bullet \equiv \frac{\epsilon_{\mu\nu}v^\nu}{P\cdot v}$, and $\epsilon_{\mu\nu}$ is the polarization tensor, which can be found in Refs. [27–29]. The distribution amplitudes can be given by [27–29]

$$\phi_T(x) = \frac{f_T}{2\sqrt{2N_c}}\phi_\parallel(x), \qquad \phi_T^t = \frac{f_T^\perp}{2\sqrt{2N_c}}h_\parallel^{(t)}(x),$$
$$\phi_T^s(x) = \frac{f_T^\perp}{4\sqrt{2N_c}}\frac{d}{dx}h_\parallel^{(s)}(x), \qquad \phi_T^T(x) = \frac{f_T^\perp}{2\sqrt{2N_c}}\phi_\perp(x),$$
$$\phi_T^v(x) = \frac{f_T}{2\sqrt{2N_c}}g_\perp^{(v)}(x), \qquad \phi_T^a(x) = \frac{f_T}{8\sqrt{2N_c}}\frac{d}{dx}g_\perp^{(a)}(x). \tag{13}$$

The asymptotic twist-2 and twist-3 distributions are [27–29]

$$\phi_{\parallel,\perp}(x) = 30x(1-x)(2x-1),$$
$$h_\parallel^{(t)}(x) = \frac{15}{2}(2x-1)(1-6x+6x^2),$$
$$h_\parallel^{(s)}(x) = 15x(1-x)(2x-1), \tag{14}$$
$$g_\perp^{(a)}(x) = 20x(1-x)(2x-1),$$
$$g_\perp^{(v)}(x) = 5(2x-1)^3.$$

These light-cone distribution amplitudes (LCDAs) of the light tensor meson are asymmetric under the interchange of momentum fractions of the quark and antiquark in the $SU(3)$ limit because of the Bose statistics [28,29].

For the $D^{(*)}$ meson, in the heavy quark limit, the two-parton LCDAs can be written as in Refs. [20,60–63],

$$\langle D(p)|q_\alpha(z)\bar{c}_\beta(0)|0\rangle = \frac{i}{\sqrt{2N_c}}\int_0^1 dx e^{ixp\cdot z}[\gamma_5(\not{P} + m_D)\phi_D(x,b)]_{\alpha\beta},$$
$$\langle D^*(p)|q_\alpha(z)\bar{c}_\beta(0)|0\rangle = -\frac{1}{\sqrt{2N_c}}\int_0^1 dx e^{ixp\cdot z}[\not{\epsilon}_L(\not{P} + m_{D^*})\phi_{D^*}^L(x,b) + \not{\epsilon}_T(\not{P} + m_{D^*})\phi_{D^*}^T(x,b)]_{\alpha\beta}. \tag{15}$$

For the distribution amplitude of the D meson, we take the same model as that used in Refs. [61–63],

$$\phi_D(x,b) = \frac{1}{2\sqrt{2N_c}}f_D 6x(1-x)[1 + C_D(1-2x)] \times \exp\left[\frac{-\omega^2 b^2}{2}\right], \tag{16}$$

with $C_D = 0.5 \pm 0.1$, $\omega = 0.1$ GeV and $f_D = 207$ MeV [64] for the $D(\bar{D})$ meson and $C_D = 0.4 \pm 0.1$, $\omega = 0.2$ GeV, and $f_{D_s} = 241$ MeV [64] for the $D_s(\bar{D}_s)$ meson. In the wave function of $D^*_{(s)}$ mesons, the $\phi_{D^*}^L$ and $\phi_{D^*}^T$ may not be related by the equation of motion. Since the mass difference of $D_{(s)}$ and $D^*_{(s)}$ is very small, in the heavy quark limit, the light quark in $D^{(*)}_{(s)}$ mesons is not sensitive to the spin and color of the heavy c or $\bar{c}$ quark. Thus, we have

$$f^T_{D^*} - f_{D^*}\frac{m_c - m_d}{m_{D^*}} \sim f_{D^*} - f^T_{D^*}\frac{m_c - m_d}{m_{D^*}} \sim o(\bar{\Lambda}/m_{D^*}). \tag{17}$$

Like Ref. [60], we adopt the same model for $\phi^L_{D^*}$ and $\phi^T_{D^*}$ as that of the D meson, and we take $f^T_{D^*} = f_{D^*}$, just for simplification. For the $D^*_{(s)}$ meson, we determine the decay constant by using the following relation based on heavy quark effective theory [65]:

$$f_{D^*_{(s)}} = \sqrt{\frac{m_{D_{(s)}}}{m^*_{D_{(s)}}}} f_{D_{(s)}}. \tag{18}$$

III. PERTURBATIVE CALCULATION

There are six types of diagrams contributing to the $B_c \to D^{(*)}T$ decays, which are shown in Fig. 1. The dominant factorizable emission-type diagrams in most other decay modes are not shown here, because they do not contribute for tensor meson emission. The second line of the figure shows the factorizable and nonfactorizable annihilation-type diagrams.

After the perturbative calculation, the decay amplitudes for the nonfactorizable emission diagrams in Figs. 1(a) and 1(b) are as follows.

(i) (V − A)(V − A) operators:

$$\mathcal{M}^{LL}_{\rm enf} = \frac{32}{3}\pi C_F m^4_{B_c}\int_0^1 d[x]\int_0^{1/\Lambda} b_1 db_1 b_2 db_2 \phi_{B_c}(x_1, b_1)\phi_T(x_2)\phi_D(x_3, b_1)\{[r_D(1-x_3) + x_1 + x_2 - 1] \times E_{\rm enf}(t_a)h_{\rm enf}(x_1, (1-x_2), x_3, b_1, b_2) - [r_D(1-x_3) + x_1 - x_2 + x_3 - 1]E_{enf}(t_b)h_{\rm enf}(x_1, x_2, x_3, b_1, b_2)\}, \tag{19}$$

(ii) (V − A)(V + A) operators:

$$\mathcal{M}^{LR}_{\rm enf} = \frac{32}{3}\pi C_F r_T m^4_{B_c}\int_0^1 d[x]\int_0^{1/\Lambda} b_1 db_1 b_2 db_2 \phi_{B_c}(x_1, b_1)\phi_D(x_3, b_1)\{[\phi^s_T(x_2)(x_1 + x_2 + r_D(x_1 + x_2 + x_3 - 2) - 1) + \phi^t_T(x_2)((x_1 + x_2)(1 + r_D) - r_D x_3 - 1)]\cdot E_{\rm enf}(t_a)h_{\rm enf}(x_1, (1-x_2), x_3, b_1, b_2) + [\phi^t_T(x_2)(x_1 - x_2 + r_D(x_1 - x_2 - x_3 + 1)) - \phi^s_T(x_2)(x_1 - x_2 + r_D(x_1 - x_2 + x_3 - 1))]\cdot E_{\rm enf}(t_b) \times h_{\rm enf}(x_1, x_2, x_3, b_1, b_2)\}, \tag{20}$$

(iii) (S − P)(S + P) operators:

$$\mathcal{M}^{SP}_{\rm enf} = -\frac{32}{3}\pi C_F m^4_{B_c}\int_0^1 d[x]\int_0^{1/\Lambda} b_1 db_1 b_2 db_2 \phi_{B_c}(x_1, b_1)\phi_T(x_2)\phi_D(x_3, b_1)[(r_D(x_3 - 1) - x_1 - x_2 - x_3 + 2) \times E_{\rm enf}(t_a)h_{enf}(x_1, (1-x_2), x_3, b_1, b_2) + (r_D(1-x_3) + x_1 - x_2)E_{enf}(t_b)h_{\rm enf}(x_1, x_2, x_3, b_1, b_2)], \tag{21}$$

where $C_F = 4/3$ is the group factor of $SU(3)_c$. The hard scale $t_{a(b)}$ and the functions $E_{\rm enf}$ and $h_{\rm enf}$ can be found in Appendix A.

Figures 1(c) and 1(d) are the factorizable annihilation diagrams, whose contributions are as follows.

(i) (V − A)(V − A) operators:

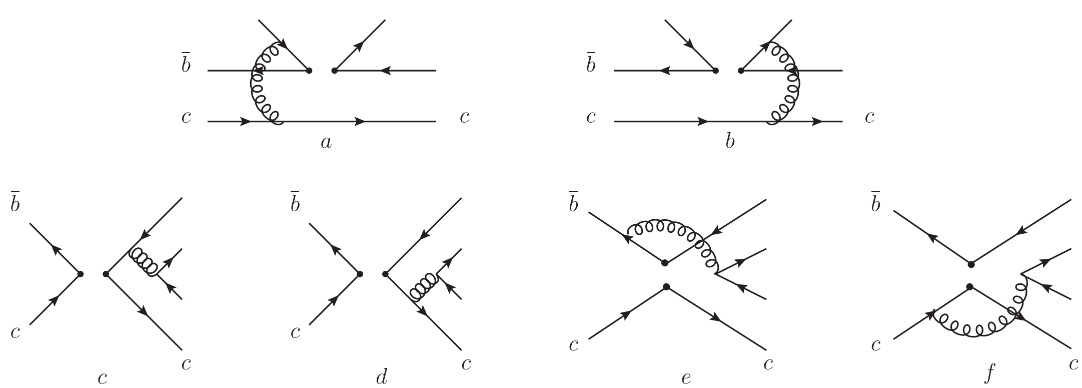

FIG. 1. Leading order Feynman diagrams contributing to the $B_c \to D^{(*)}T$ decays in PQCD. (a, b) the nonfactorizable emission diagrams, (c, d) the factorizable annihilation diagrams, and (e, f) the nonfactorizable annihilation diagrams.

$$\mathcal{M}_{af}^{LL} = 8\sqrt{\frac{2}{3}}C_F\pi f_{B_c}m_{B_c}^4\int_0^1 dx_2dx_3\int_0^{1/\Lambda} b_2db_2b_3db_3\phi_D(x_3,b_3)\{[2\phi_T^s(x_2)r_Dr_T(x_3+1)+\phi_T(x_2)x_3] \times E_{af}(t_c)h_{af1}(x_2,x_3,b_2,b_3)+[\phi_T(x_2)(2r_cr_D-x_2)+r_T(-\phi_T^t(x_2)(2r_D(x_2-1)+r_c) + \phi_T^s(x_2)(-2(x_2+1)r_D+r_c))]E_{af}(t_d)h_{af2}(x_2,x_3,b_2,b_3)\}, \tag{22}$$

(ii) (S − P)(S + P) operators:

$$\mathcal{M}_{af}^{SP} = -16\sqrt{\frac{2}{3}}C_Ff_{B_c}\pi m_{B_c}^4\int_0^1 dx_2dx_3\int_0^{1/\Lambda}\phi_D(x_3,b_3)[(2\phi_T^s(x_2)r_T+r_D\phi_T(x_2)x_3)E_{af}(t_c)h_{af1}(x_2,x_3,b_2,b_3) + (\phi_T(x_2)(2r_D-r_c)+r_T(\phi_T^s(x_2)(x_2-4r_Dr_c)-\phi_T^t(x_2)x_2))\cdot E_{af}(t_d)h_{af2}(x_2,x_3,b_2,b_3)], \tag{23}$$

with $r_c = m_c/m_{B_c}$. m_c is the mass of the c quark. $t_{c(d)}$, E_{af}, and $h_{af1(2)}$ are also listed in Appendix A.

The last two diagrams in Fig. 1 are the nonfactorizable annihilation diagrams, whose contributions are as follows.

(i) (V − A)(V − A) operators:

$$\mathcal{M}_{anf}^{LL} = -\frac{32}{3}C_F\pi m_{B_c}^4\int_0^1 d[x]\int_0^{1/\Lambda} b_1db_1b_2db_2\phi_{B_c}(x_1,b_1)\phi_D(x_3,b_2)\{[\phi_T(x_2)(1-x_1-x_2-r_b) - r_Tr_D(\phi_T^t(x_2)(x_1+x_2-x_3)+\phi_T^s(x_2)(x_1+x_2+x_3-2+4r_b))]E_{anf}(t_e)h_{anf1}(x_1,x_2,x_3,b_1,b_2) + [\phi_T^s(x_2)r_Dr_T(-x_1+x_2+x_3+4r_c)+\phi_T^t(x_2)r_Dr_T(x_1-x_2+x_3)+\phi_T(x_2)(x_3+r_c)] \times E_{anf}(t_f)h_{anf2}(x_1,x_2,x_3,b_1,b_2)\}, \tag{24}$$

(ii) (V − A)(V + A) operators:

$$\mathcal{M}_{anf}^{LR} = -\frac{32}{3}C_F\pi m_{B_c}^4\int_0^1 d[x]\int_0^{1/\Lambda} b_1db_1b_2db_2\phi_{B_c}(x_1,b_1)\phi_D(x_3,b_2)\{[-(\phi_T^t(x_2)+\phi_T^s(x_2))r_T(x_1+x_2-1-r_b) + \phi_T(x_2)r_D(x_3-1-r_b)]\cdot E_{anf}(t_e)h_{anf1}(x_1,x_2,x_3,b_1,b_2)+[-(\phi_T^s(x_2)+\phi_T^t(x_2))r_T(x_1-x_2+r_c) - \phi_T(x_2)r_D(x_3-r_c)]\cdot E_{anf}(t_f)h_{anf2}(x_1,x_2,x_3,b_1,b_2)\}, \tag{25}$$

with $r_b = m_b/m_{B_c}$. $t_{e(f)}$, E_{anf}, and $h_{anf1(2)}$ are also listed in Appendix A.

With the factorization formulas obtained above, for these $B_c \to DT$ decays, the total amplitudes containing the Wilson coefficients and CKM elements can be written as

$$\mathcal{A}(B_c\to a_2^+D^0) = \frac{G_F}{\sqrt{2}}\{V_{ub}^*V_{ud}\mathcal{M}_{\rm enf}^{LL}C_1+V_{cb}^*V_{cd}(\mathcal{M}_{af}^{LL}a_1+\mathcal{M}_{anf}^{LL}C_1)-V_{tb}^*V_{td}[\mathcal{M}_{enf}^{LL}(C_3+C_9)+\mathcal{M}_{\rm enf}^{LR}(C_5+C_7) + \mathcal{M}_{af}^{LL}(a_4+a_{10})+\mathcal{M}_{af}^{SP}(a_6+a_8)+\mathcal{M}_{anf}^{LL}(C_3+C_9)+\mathcal{M}_{anf}^{LR}(C_5+C_7)]\}, \tag{26}$$

$$\mathcal{A}(B_c\to K_2^{*+}D^0) = \mathcal{A}(B_c\to a_2^+D^0)\,|_{V_{ud}\to V_{us},V_{cd}\to V_{cs},V_{td}\to V_{ts},a_2^+\to K_2^{*+}}, \tag{27}$$

$$\mathcal{A}(B_c\to a_2^0D^+) = \frac{G_F}{\sqrt{2}}\frac{1}{\sqrt{2}}\{V_{ub}^*V_{ud}\mathcal{M}_{\rm enf}^{LL}C_2-V_{cb}^*V_{cd}(\mathcal{M}_{af}^{LL}a_1+\mathcal{M}_{anf}^{LL}C_1)-V_{tb}^*V_{td}[\mathcal{M}_{enf}^{LL}(-C_3+3a_{10}/2) + \mathcal{M}_{\rm enf}^{LR}(-C_5+C_7/2)+\mathcal{M}_{enf}^{SP}(3C_8/2)-\mathcal{M}_{af}^{LL}(a_4+a_{10})-\mathcal{M}_{af}^{SP}(a_6+a_8)-\mathcal{M}_{anf}^{LL}(C_3+C_9) - \mathcal{M}_{anf}^{LR}(C_5+C_7)]\}, \tag{28}$$

$$\mathcal{A}(B_c \to K_2^{*0} D^+) = \frac{G_F}{\sqrt{2}}\{V_{cb}^* V_{cs}(\mathcal{M}_{af}^{LL} a_1 + \mathcal{M}_{anf}^{LL} C_1) - V_{tb}^* V_{ts}[\mathcal{M}_{\rm enf}^{LL}(C_3 - C_9/2) + \mathcal{M}_{enf}^{LR}(C_5 - C_7/2) + \mathcal{M}_{af}^{LL}(a_4 + a_{10}) + \mathcal{M}_{af}^{SP}(a_6 + a_8) + \mathcal{M}_{anf}^{LL}(C_3 + C_9) + \mathcal{M}_{anf}^{LR}(C_5 + C_7)]\}, \tag{29}$$

$$\mathcal{A}(B_c \to f_2^q D^+) = \frac{G_F}{\sqrt{2}}\frac{1}{\sqrt{2}}\{V_{ub}^* V_{ud}\mathcal{M}_{\rm enf}^{LL} C_2 + V_{cb}^* V_{cd}(\mathcal{M}_{af}^{LL} a_1 + \mathcal{M}_{anf}^{LL} C_1) - V_{tb}^* V_{td}[\mathcal{M}_{\rm enf}^{LL}(C_3 + 2C_4 - C_9/2 + C_{10}/2) + \mathcal{M}_{\rm enf}^{LR}(C_5 - C_7/2) + \mathcal{M}_{enf}^{SP}(2C_6 + C_8/2) + \mathcal{M}_{af}^{LL}(a_4 + a_{10}) + \mathcal{M}_{af}^{SP}(a_6 + a_8) + \mathcal{M}_{anf}^{LL}(C_3 + C9) + \mathcal{M}_{anf}^{LR}(C_5 + C_7)]\}, \tag{30}$$

$$\mathcal{A}(B_c \to f_2^s D^+) = \frac{G_F}{\sqrt{2}}\{-V_{tb}^* V_{td}[\mathcal{M}_{\rm enf}^{LL}(C_4 - C_{10}/2) + \mathcal{M}_{\rm enf}^{SP}(C_6 - C_8/2)]\}, \tag{31}$$

$$\mathcal{A}(B_c \to a_2^0 D_s^+) = \frac{G_F}{\sqrt{2}}\frac{1}{\sqrt{2}}\{V_{ub}^* V_{us}\mathcal{M}_{\rm enf}^{LL} C_2 - V_{tb}^* V_{ts}[\mathcal{M}_{\rm enf}^{LL} 3C_{10}/2 + \mathcal{M}_{\rm enf}^{SP} 3C_8/2]\}, \tag{32}$$

$$\mathcal{A}(B_c \to \bar{K}_2^{*0} D_s^+) = \frac{G_F}{\sqrt{2}}\{V_{cb}^* V_{cd}(\mathcal{M}_{af}^{LL} a_1 + \mathcal{M}_{anf}^{LL} C_1) - V_{tb}^* V_{td}[\mathcal{M}_{af}^{LL}(a_4 + a_{10}) + \mathcal{M}_{af}^{SP}(a_6 + a_8) + \mathcal{M}_{anf}^{LL}(C_3 + C_9) + \mathcal{M}_{anf}^{LR}(C_5 + C_7)]\}, \tag{33}$$

$$\mathcal{A}(B_c \to f_2^q D_s^+) = \frac{G_F}{\sqrt{2}}\frac{1}{\sqrt{2}}\{V_{ub}^* V_{us}\mathcal{M}_{\rm enf}^{LL} C_2 - V_{tb}^* V_{ts}[\mathcal{M}_{\rm enf}^{LL}(2C_4 + C_{10}/2) + \mathcal{M}_{\rm enf}^{SP}(2C_6 + C_8/2)]\}, \tag{34}$$

$$\mathcal{A}(B_c \to f_2^s D_s^+) = \frac{G_F}{\sqrt{2}}\{V_{cb}^* V_{cs}(\mathcal{M}_{af}^{LL} a_1 + \mathcal{M}_{anf}^{LL} C_1) - V_{tb}^* V_{ts}[\mathcal{M}_{\rm enf}^{LR}(C_5 - C_7/2) + \mathcal{M}_{\rm enf}^{LL}(C_3 + C_4 - C_9/2 - C_{10}/2) + \mathcal{M}_{\rm enf}^{SP}(C_6 - C_8/2) + \mathcal{M}_{af}^{LL}(a_4 + a_{10}) + \mathcal{M}_{af}^{SP}(a_6 + a_8) + \mathcal{M}_{anf}^{LL}(C_3 + C_9) + \mathcal{M}_{anf}^{LR}(C_5 + C_7)]\}. \tag{35}$$

From Eq. (42), we know that

$$\mathcal{A}(B_c \to D^{(*)} f_2) = \mathcal{A}(B_c \to D^{(*)} f_2^q)\cos\theta + \mathcal{A}(B_c \to D^{(*)} f_2^s)\sin\theta, \tag{36}$$

$$\mathcal{A}(B_c \to D^{(*)} f_2') = \mathcal{A}(B_c \to D^{(*)} f_2^q)\sin\theta - \mathcal{A}(B_c \to D^{(*)} f_2^s)\cos\theta, \tag{37}$$

with $\theta = 7.8°$.

The amplitudes of $B_c \to D^* T$ decay can be decomposed as

$$\mathcal{A}(\epsilon_D, \epsilon_T) = i\mathcal{A}^N + i(\epsilon_D^{T*}\cdot\epsilon_T^{T*})\mathcal{A}^s + (\epsilon_{\mu\nu\alpha\beta} n^\mu v^\nu \epsilon_D^{T*\alpha}\epsilon_T^{T*\beta})\mathcal{A}^p, \tag{38}$$

where $\mathcal{A}^N$ contains the contribution from the longitudinal polarizations, while $\mathcal{A}^s$ and $\mathcal{A}^p$ represent the transversely polarized contributions. ϵ_D^T is the transverse polarization vector of the D^* meson, and ϵ_T^T is the vector used to construct the polarization tensors of the tensor meson. For each decay process of $B_c \to D^* T$, the amplitudes $\mathcal{A}^N$, $\mathcal{A}^s$, and $\mathcal{A}^p$ have the same structures as Eqs. (26)–(35), respectively. The factorization formulas for the longitudinal and transverse polarizations for the $B_c \to D^* T$ decays are listed in Appendix B.

IV. NUMERICAL RESULTS AND DISCUSSIONS

The decay width of a B_c meson at rest decaying into D and T mesons is

$$\Gamma(B_c \to DT) = \frac{|\vec{P}|}{8\pi m_{B_c}^2}|\mathcal{A}(B_c \to DT)|^2, \tag{39}$$

where the momentum of the final state particle is given by

$$|\vec{P}| = \frac{1}{2m_{B_c}}\sqrt{[m_{B_c}^2 - (m_D + m_T)^2][m_{B_c}^2 - (m_D - m_T)^2]}. \tag{40}$$

The masses and decay constants of tensor mesons needed in the numerical calculations are summarized in Table I. Other parameters such as the QCD scale (GeV),

TABLE I. The masses and decay constants of light tensor mesons [28,66,67].

Tensor [mass (MeV)]	f_T (MeV)	$f_T^\perp$ (MeV)
$f_2(1270)$	102 ± 6	117 ± 25
$f_2'(1525)$	126 ± 4	65 ± 12
$a_2(1320)$	107 ± 6	105 ± 21
$K_2^*(1430)$	118 ± 5	77 ± 14

the mass (GeV), and the lifetime and decay constant of the B_c meson are

$$\Lambda_{\overline{\rm MS}}^{f=4} = 0.25, \quad m_{B_c} = 6.286, \quad f_{B_c} = 0.489, \quad \tau_{B_c} = 0.46\ \text{ps}, \quad \omega_{B_c} = 0.6, \quad m_b = 4.8, \quad m_c = 1.5. \tag{41}$$

For the CKM matrix elements, we adopt the Wolfenstein parametrization, taking $A = 0.808$, $\lambda = 0.2253$, $\bar{\rho} = 0.132$, and $\bar{\eta} = 0.341$ [48].

Like the $\eta - \eta'$ mixing, the isoscalar tensor states $f_2(1270)$ and $f_2'(1525)$ also have a mixing, given by

$$f_2 = f_2^q \cos\theta + f_2^s \sin\theta, \quad f_2' = f_2^q \sin\theta - f_2^s \cos\theta, \tag{42}$$

with $f_2^q = \frac{1}{\sqrt{2}}(u\bar{u} + d\bar{d})$, $f_2^s = s\bar{s}$, and the mixing angle $\theta = 5.8°$ [68], $7.8°$ [69], or $(9 \pm 1)°$ [48].

For $B_c \to D^* T$ decays, with three kinds of polarization amplitudes, the decay width can be written as

$$\Gamma(B_c \to D^* T) = \frac{|\vec{P}|}{8\pi m_B^2}[|\mathcal{A}^N|^2 + 2(|\mathcal{A}^s|^2 + |\mathcal{A}^p|^2)]. \tag{43}$$

The CP averaged branching ratios and the direct CP asymmetries for the considered decay modes using the PQCD approach are summarized in Tables II and III. The numerical results obtained from perturbative calculations are sensitive to many parameters. For the theoretical uncertainties in our calculations, we estimated three kinds: The first errors are caused by the hadronic parameters of meson wave functions, such as the decay constants and the shape parameters of light tensor mesons and charmed mesons, which are given in Sec. II and in this section. The second errors are estimated from the uncertainty of $\Lambda_{\rm QCD} = (0.25 \pm 0.05)$ GeV and the choice of the hard scales varying from $0.8t$ to $1.2t$, which characterize the unknown next-to-leading order QCD corrections. The third error is from the uncertainties of the CKM matrix elements. It is easy to see that the most important theoretical uncertainty is caused by the nonperturbative hadronic parameters, which can be improved by experiments. For these considered decays, the dominant contributions are from the annihilation-type diagrams, which do not depend heavily on the distribution amplitude of the B_c meson. The B_c meson wave function, especially the decay constant and momentum fraction of the c quark, is an overall factor with less than 10% uncertainty for the branching ratios of all channels. So we do not include this small uncertainty in the numerical tables.

It is easy to find that there are large theoretical uncertainties in any of the individual decay channel calculations, mostly due to the shortage of the tensor meson property and the distribution amplitude of the B_c meson. In order to reduce the effects of the choice of input parameters, we define the ratios of the branching ratios between relevant decay modes:

$$\frac{{\rm Br}(B_c \to D^{(*)0} a_2^+)}{{\rm Br}(B_c \to D^{(*)+} a_2^0)} \sim 2, \tag{44}$$

$$\frac{{\rm Br}(B_c \to D^{(*)+} K_2^{*0})}{{\rm Br}(B_c \to D^{(*)0} K_2^{*+})} \sim \frac{{\rm Br}(B_c \to D^{(*)+} a_2^0)}{{\rm Br}(B_c \to D^{(*)+} f_2)} \sim 1, \tag{45}$$

$$\frac{{\rm Br}(B_c \to D_s^{(*)+} \bar{K}_2^{*0})}{{\rm Br}(B_c \to D_s^{(*)+} f_2')} \sim \left(\frac{f_{K_2^*}^T (f_{K_2^*}) V_{cd}}{f_{f_2'}^T (f_{f_2'}) V_{cs}}\right)^2 \sim \frac{1}{20}, \tag{46}$$

$$\frac{{\rm Br}(B_c \to D^+ f_2)}{{\rm Br}(B_c \to D^+ K_2^{*0})} \sim \left(\frac{1}{\sqrt{2}} \frac{f_{f_2}^T V_{cd}}{f_{K_2^*}^T V_{cs}}\right)^2 \sim \frac{1}{20}, \tag{47}$$

$$\frac{{\rm Br}(B_c \to D^{*+} f_2)}{{\rm Br}(B_c \to D^{*+} K_2^{*0})} \sim \left(\frac{1}{\sqrt{2}} \frac{f_{f_2} V_{cd}}{f_{K_2^*} V_{cs}}\right)^2 \sim \frac{1}{40}. \tag{48}$$

It is obvious that any significant deviation from the above relations will be a test of the factorization or signal of new physics.

TABLE II. Branching ratios (unit: 10^{-6}) and direct CP asymmetries (unit: %) of $B_c \to DT$ decays calculated in the PQCD approach.

Decay modes	Class	Branching ratios	$A_{CP}^{\rm dir}$
$B_c \to D^0 a_2^+$	A	$2.17^{+0.83+0.17+0.20}_{-0.71-0.17-0.18}$	$6.47^{+1.35+5.33+0.00}_{-1.15-1.59-0.74}$
$B_c \to D^0 K_2^{*+}$	A	$31.9^{+10.3+2.81+0.86}_{-8.76-2.86-0.54}$	$-0.44^{+0.13+0.10+0.10}_{-0.15-0.22-0.02}$
$B_c \to D^+ a_2^0$	A	$1.10^{+0.42+0.09-0.23}_{-0.36-0.11-0.26}$	$18.2^{+4.73+10.2+0.00}_{-3.77-4.65-2.30}$
$B_c \to D^+ K_2^{*0}$	A	$31.6^{+11.3+3.10+1.01}_{-9.69-2.13-0.63}$	0.0
$B_c \to D^+ f_2$	A	$1.51^{+0.58+0.12+0.14}_{-0.48-0.09-0.16}$	$-9.71^{+3.45+4.09+2.70}_{-3.97-5.21-1.59}$
$B_c \to D^+ f_2'$	A, P	$0.012^{+0.006+0.004+0.001}_{-0.005-0.003-0.002}$	$-47.5^{+16.9+10.2+9.7}_{-20.1-4.8-9.7}$
$B_c \to D_s^+ a_2^0$	C	$0.0047^{+0.0011+0.0016+0.0006}_{-0.0007-0.0012-0.0004}$	$-2.04^{+0.34+0.62+0.58}_{-0.37-1.29-0.28}$
$B_c \to D_s^+ \bar{K}_2^{*0}$	A	$1.90^{+0.67+0.20+0.09}_{-0.59-0.22-0.07}$	$-1.00^{+0.76+0.72+0.00}_{-0.82-0.50-0.03}$
$B_c \to D_s^+ f_2$	A, P	$1.87^{+0.43+0.45+0.06}_{-0.40-0.44-0.06}$	$2.53^{+0.51+1.45+0.10}_{-0.48-0.72-0.51}$
$B_c \to D_s^+ f_2'$	A	$40.9^{+11.9+4.32+1.20}_{-10.7-4.17-0.81}$	$-0.11^{+0.02+0.03+0.02}_{-0.02-0.06-0.00}$

TABLE III. Branching ratios (unit: 10^{-6}), direct CP asymmetries (unit: %), and the percentage of transverse polarizations R_T (unit: %) of $B_c \to D^* T$ decays calculated in the PQCD approach.

Decay modes	Class	Branching ratio	$A_{CP}^{\rm dir}$	R_T
$B_c \to D^{*0} a_2^+$	A	$7.34^{+2.05+0.99+0.24}_{-1.75-0.49-0.12}$	$5.02^{+0.54+1.34+0.07}_{-0.54-1.37-0.51}$	69.8
$B_c \to D^{*0} K_2^*$	A	$151^{+30.1+18.2+4.69}_{-26.5-10.5-3.00}$	$-0.15^{+0.02+0.05+0.03}_{-0.02-0.08-0.06}$	82.5
$B_c \to D^{*+} a_2^0$	A	$3.75^{+1.05+0.49+0.05}_{-0.88-0.23-0.02}$	$7.94^{+1.25+4.07+0.34}_{-1.23-3.87-1.26}$	68.2
$B_c \to D^{*+} K_2^{*0}$	A	$158^{+30.6+16.0+0.00}_{-28.5-14.9-13.4}$	0.0	80.3
$B_c \to D^{*+} f_2$	A	$3.38^{+1.03+0.43+0.33}_{-0.90-0.22-0.26}$	$-2.47^{+1.01+1.55+0.82}_{-1.11-5.11-0.00}$	69.7
$B_c \to D^{*+} f_2'$	A	$0.091^{+0.025+0.011+0.009}_{-0.023-0.008-0.009}$	$-5.62^{+1.40+4.63+0.29}_{-1.55-6.30-0.00}$	45.3
$B_c \to D_s^{*+} a_2^0$	C	$0.0051^{+0.0008+0.0022+0.0006}_{-0.0006-0.0015-0.0004}$	$-3.81^{+0.24+0.52+1.09}_{-0.17-0.81-0.51}$	12.7
$B_c \to D_s^{*+} \bar{K}_2^{*0}$	A	$8.94^{+1.70+0.79+0.45}_{-1.58-0.92-0.28}$	$2.30^{+0.24+0.85+0.01}_{-0.14-0.45-0.01}$	82.0
$B_c \to D_s^{*+} f_2$	A	$3.60^{+0.42+0.61+0.11}_{-0.38-0.51-0.08}$	$2.09^{+0.15+0.39+0.10}_{-0.16-0.41-0.40}$	98.4
$B_c \to D_s^{*+} f_2'$	A	$190^{+30.5+19.6+6.14}_{-28.1-13.2-3.88}$	$-0.036^{+0.004+0.011+0.008}_{-0.003-0.012-0.001}$	89.5

For all considered $B_c \to D^{(*)} T$ decays, the factorizable emission diagrams do not contribute, because the tensor meson cannot be produced through local $(V \pm A)$ current or $(S \pm P)$ density. But these decays can obtain contributions from nonfactorizable and annihilation diagrams. In fact, most of these decays are dominated by the W annihilation diagrams (A), as classified in the tables. There are only four decay channels, which are dominated by the color suppressed (C) or penguin (P) diagrams with almost negligible branching ratios. As we know, usually the annihilation diagrams are power suppressed compared with the emission diagrams in B decays. This is also shown in the first channel of Table III in Ref. [26] for the $B_c \to D^0 \rho^+$ decay, where the emission diagram (T) is indeed dominant. If the ρ meson is replaced by the corresponding tensor meson a_2^+, we get a smaller branching ratio of $B_c \to D^0 a_2^+$, since the emission of a tensor meson is prohibited. But for those penguin dominant decay channels with a $b \to s$ transition, such as $B_c \to D^0 K^{*+}$ and $D^+ K^{*0}$, the contributions from the annihilation-type diagrams are enhanced by the large CKM elements $V_{cs(d)}$ and large Wilson coefficient a_1. The annihilation diagrams are at the same order of magnitude as penguin emission diagrams but with a relative minus sign [26]. These penguin "dominant" decays thus have smaller branching ratios than tree dominant $B_c \to D^0 \rho^+$ decays, unlike the B^+ decays. In our considered B_c decays with missing tensor meson emission diagrams, the corresponding $B_c \to D^0 K_2^{*+}$ and $D^+ K_2^{*0}$ decays have much larger branching ratios shown in Table II due to the large annihilation contribution alone. Therefore, it is interesting that the B_c meson decays to tensor final states with branching ratios as large as 10^{-4} will be easier for experiments to search than the corresponding decays with vector final states.

As stated in Refs. [3,4], the LHC experiment, specifically the LHCb, can produce around 5×10^{10} B_c events each year. The B_c decays with a decay rate at the level of 10^{-6} can be detected with a good precision at LHC experiments [14]. On the basis of our predictions, some of these $B_c \to D^{(*)} T$ decays with large branching ratios can be observed in the experiments soon. The predicted branching ratio of $B_c \to D^+ K_2^{*0}$ in this work is about 3×10^{-5}. The branching ratios of D^+ and K_2^{*0} decays with charged final states are 10% ($D^+ \to K^- \pi^+ \pi^+$) [70] and 25% [$\mathcal{B}(K_2^{*0} \to K\pi) = (49.9 \pm 1.2)\%$], respectively. Assuming a total efficiency of 1% [70], one can expect about dozens of events. For $B_c \to D_s^+ f_2'$, the predicted branching ratio is 4×10^{-5}. The branching ratios of D_s^+ and f_2' decays with charged final states are about 6% ($D_s^+ \to K^+ K^- \pi^+$) and 45% [$\mathcal{B}(f_2' \to K\bar{K}) = (88.7 \pm 2.2)\%$], respectively. Assuming a total efficiency of 1%, one can expect about 100 events. They are the most promising channels to be measured in the forthcoming experiments. For $B_c \to D^{*+} K_2^{*0}$ and $B_c \to D_s^{*+} f_2'$, the $D_{(s)}^*$ will decay to $D_{(s)}$ first. The situation is similar. Because the branching ratios of these two B_c decays are of order 10^{-4}, we also expect that they will be measured by the ongoing LHCb experiments. On the other hand, since the contributions from penguin operators are so small compared with the contributions from tree operators, the direct CP asymmetries are all very small except for $B_c \to D^+ f_2'$. For $B_c \to D^+ f_2'$ decay, the tree contributions from the f_2^q term are suppressed by the mixing angle [see (42)], to be at the same level with penguin contributions from the f_2^s term. The interference is sizable; thus, the direct CP asymmetry is around -50%. Unfortunately, this decay channel is not accessible easily by current experiments due to a too-small branching ratio.

For $B_c \to D^* T$ decays, we also calculate the percentage of the transverse polarization R_T, which can be described as

$$R_T = \frac{2(|\mathcal{A}^s|^2 + |\mathcal{A}^p|^2)}{|\mathcal{A}^N|^2 + 2(|\mathcal{A}^s|^2 + |\mathcal{A}^p|^2)}. \tag{49}$$

Usually, from naive factorization expectation, the longitudinal polarizations dominate the branching ratios of

B decays. However, from the numerical results shown in Table III, one can see that the transverse polarized contributions are about at the same level as the longitudinal polarized contributions. In fact, from Eqs. (B4) and (B14), we can find that, although the transverse polarized contributions are power suppressed, they are also about at the same level as the longitudinal polarized contributions because the two factorizable annihilation diagrams strongly cancel each other in the longitudinally polarized case. As a result, for these W-annihilation-diagram dominant decays, the percentages of the transverse polarization are around 70% or even bigger. This large percentage can be understood as follows [71]: We know that the light quark and the antiquark created from hard gluons are left-handed or right-handed with equal opportunity. What is more, the c quark from the four-quark operator is right-handed. So the D^* meson can be longitudinally polarized or transversely polarized with polarization $\lambda = -1$. Because the antiquark from the four-quark operator is right-handed, and the quark produced from the hard gluon can be either left-handed or right-handed, with the additional contribution from the orbital angular momentum, the tensor meson can be longitudinally polarized or transversely polarized with polarization $\lambda = -1$. As a result, the transverse polarization can become so large, with additional interference from other diagrams. For $B_c \to D_s^{*+} f_2$, the longitudinal contributions from color suppressed diagrams and W annihilation diagrams strongly cancel each other, while the transverse contributions can not cancel because the transverse contributions from color suppressed tree diagrams are too small. As a result, the ratio of transverse polarizations becomes as large as 98.4%. But for the color suppressed dominant $B_c \to D_s^{*+} a_2^0$ decay, according to the power counting rules in the factorization assumption, the longitudinal contributions should be dominant due to the quark helicity analysis [72,73]. The ratio is only around 10%.

V. SUMMARY

In this paper, we investigate $B_c \to D^{(*)}T$ decays within the framework of the perturbative QCD approach. We estimate and calculate the contributions of different diagrams in the leading order approximation of m_D/m_{B_c} expansion. Most of these decays are dominated by the W annihilation diagrams, which are only calculable in the pQCD approach. Since the emission of a tensor meson is prohibited, the cancellation between the penguin emission diagram and the tree annihilation diagram that occurred in the $B_c \to D^{(*)}V$ decays [26] does not exist here. We predict one-order-magnitude larger branching ratios for $B_c \to D^{(*)}K_2^*$ decays than the corresponding $B_c \to D^{(*)}K^*$ decays. The $B_c \to D^{(*)}K_2^*$ decays are thus easier to detect in the ongoing LHCb experiments. These samples of B_c decays would provide an opportunity to study properties of the B_c meson and the factorization theorem of decay modes with a tensor meson emitted. Most of the direct CP asymmetries are very small because the penguin contributions are too small compared with the tree annihilation contributions. We also predict large ratios of transverse polarizations, around 70% or even bigger for those W annihilation dominant decays.

ACKNOWLEDGMENTS

We are very grateful to Xin Liu for helpful discussions. This work is partly supported by the National Science Foundation of China under Grants No. 11228512, No. 11235005, and No. 11075168, and the Project of Knowledge Innovation Program (PKIP) of Chinese Academy of Sciences, Grant No. KJCX2.YW.W10.

APPENDIX A: RELATED HARD FUNCTIONS

In this appendix, we summarize the functions that appear in the analytic formulas in Sec. III. The first two diagrams in Fig. 1 are nonfactorizable emission diagrams, whose hard scales $t_{a(b)}$ can be determined by

$$t_a = \max\left\{\sqrt{(x_1 - r_D^2)(1 - x_3)}m_{B_c}, \sqrt{|(x_3 - 1)[(1 - r_D^2)(1 - x_2) - (x_1 - r_D^2)]|}m_{B_c}, 1/b_1, 1/b_2\right\}, \tag{A1}$$

$$t_b = \max\left\{\sqrt{(x_1 - r_D^2)(1 - x_3)}m_{B_c}, \sqrt{|(x_3 - 1)[(1 - r_D^2)x_2 - (x_1 - r_D^2)]|}m_{B_c}, 1/b_1, 1/b_2\right\}. \tag{A2}$$

The evolution factors $E_{\mathrm{enf}}(t_a)$ and $E_{\mathrm{enf}}(t_b)$ in the analytic formulas (see Sec. III) are given by

$$E_{\mathrm{enf}}(t) = \alpha_s(t)\exp[-S_{B_c}(t) - S_T(t) - S_D(t)]|_{b_1=b_3}. \tag{A3}$$

The Sudakov exponents are defined as

$$S_{B_c}(t) = s\left(x_1\frac{m_{B_c}}{\sqrt{2}}, b_1\right) + \frac{5}{3}\int_{1/b_1}^{t}\frac{d\bar{\mu}}{\bar{\mu}}\gamma_q(\alpha_s(\bar{\mu})), \tag{A4}$$

$$S_D(t) = s\left(x_3\frac{m_{B_c}}{\sqrt{2}}, b_3\right) + 2\int_{1/b}^{t}\frac{d\bar{\mu}}{\bar{\mu}}\gamma_q(\alpha_s(\bar{\mu})), \tag{A5}$$

$$S_T(t) = s\left(x_2\frac{m_{B_c}}{\sqrt{2}}, b_2\right) + s\left((1-x_2)\frac{m_{B_c}}{\sqrt{2}}, b_2\right) + 2\int_{1/b}^{t}\frac{d\bar{\mu}}{\bar{\mu}}\gamma_q(\alpha_s(\bar{\mu})), \tag{A6}$$

where the $s(Q, b)$ can be found in Appendix A of Ref. [50]. The function $h_{\rm enf}$ can be given as

$$h_{\rm enf}(x_1, x_2, x_3, b_1, b_2) = [\theta(b_2 - b_1)K_0(D_0 m_{B_c} b_2)I_0(D_0 m_{B_c} b_1) + \theta(b_1 - b_2)K_0(D_0 m_{B_c} b_1)I_0(D_0 m_{B_c} b_2)] \cdot \begin{cases} \frac{i\pi}{2}H_0^{(1)}(\sqrt{|D^2|}m_B b_2), & D^2 < 0; \\ K_0(D m_B b_2), & D^2 > 0, \end{cases} \tag{A7}$$

with

$$D_0^2 = (1 - x_3)(x_1 - r_D^2), \tag{A8}$$

$$D^2 = (x_3 - 1)[(1 - r_D^2)x_2 - (x_1 - r_D^2)]. \tag{A9}$$

For the rest of the diagrams, the related functions are summarized as follows:

$$\begin{aligned} t_c &= \max\left\{\sqrt{(1-r_D^2)x_3}m_{B_c}, 1/b_2, 1/b_3\right\}, \\ t_d &= \max\left\{\sqrt{x_2x_3(1-r_D^2)}m_{B_c}, \sqrt{(1-r_D^2)x_2 + r_D^2 - r_c^2}m_{B_c}, 1/b_2, 1/b_3\right\}, \end{aligned} \tag{A10}$$

$$E_{af}(t) = \alpha_s(t)\exp[-S_T(t) - S_D(t)], \tag{A11}$$

$$\begin{aligned} h_{af1}(x_2, x_3, b_2, b_3) = {} & \left(\frac{i\pi}{2}\right)^2 H_0^{(1)}\left(\sqrt{x_2x_3(1-r_D^2)}m_{B_c}b_2\right)\Big[\theta(b_2 - b_3)H_0^{(1)}\left(\sqrt{F_1^2}m_{B_c}b_2\right)J_0\left(\sqrt{F_1^2}m_{B_c}b_3\right) \\ & + \theta(b_3 - b_2)H_0^{(1)}\left(\sqrt{F_1^2}m_{B_c}b_3\right)J_0\left(\sqrt{F_1^2}m_{B_c}b_2\right)\Big]\cdot S_t(x_3) \end{aligned} \tag{A12}$$

$$h_{af2}(x_2, x_3, b_2, b_3) = h_{af1}(x_2, x_3, b_2, b_3)|_{b_2 \longleftrightarrow b_3, F_1^2 \to F_2^2}, \tag{A13}$$

with

$$F_1^2 = (1 - r_D^2)x_3, \tag{A14}$$

$$F_2^2 = (1 - r_D^2)x_2 + r_D^2 - r_c^2. \tag{A15}$$

The $S_t(x)$ is the jet function with the expression [57]

$$S_t(x) = \frac{2^{1+2c}\Gamma(3/2 + c)}{\sqrt{\pi}\Gamma(1 + c)}[x(1 - x)]^c, \tag{A16}$$

where $c = 0.3$. For the nonfactorizable diagrams, we omit the $S_t(x)$, because it provides a very small numerical effect to the amplitude [74],

$$\begin{aligned} t_e &= \max\left\{\sqrt{x_2x_3(1-r_D^2)}m_{B_c}, \sqrt{|r_b^2 - (1-x_3)(1-x_1-(1-r_D^2)x_2)|}m_{B_c}, 1/b_1, 1/b_2\right\}, \\ t_f &= \max\left\{\sqrt{x_2x_3(1-r_D^2)}m_{B_c}, \sqrt{|r_c^2 + x_3(x_1-(1-r_D^2)x_2)|}m_{B_c}, 1/b_1, 1/b_2\right\}, \end{aligned} \tag{A17}$$

$$E_{anf} = \alpha_s(t)\cdot\exp[-S_B(t) - S_T(t) - S_D(t)]\,|_{b_2=b_3}, \tag{A18}$$

$$h_{anfj}(x_1, x_2, x_3, b_1, b_2) = \frac{i\pi}{2}[\theta(b_1 - b_2)H_0^{(1)}(Gm_{B_c}b_1)J_0(Gm_{B_c}b_2) + \theta(b_2 - b_1)H_0^{(1)}(Gm_{B_c}b_2)J_0(Gm_{B_c}b_1)] \times \begin{cases} \frac{i\pi}{2}H_0^{(1)}\left(\sqrt{|G_j^2|}m_{B_c}b_1\right), & G_j^2 < 0, \\ K_0(G_j m_{B_c}b_1), & G_j^2 > 0, \end{cases} \tag{A19}$$

with $j = 1, 2$.

$$G^2 = x_2x_3(1 - r_D^2), \tag{A20}$$

$$G_1^2 = r_b^2 - (1 - x_3)(1 - x_1 - (1 - r_D^2)x_2), \tag{A21}$$

$$G_2^2 = r_c^2 + x_3(x_1 - (1 - r_D^2)x_2). \tag{A22}$$

APPENDIX B: FACTORIZATION FORMULAS FOR $B_c \to D^*T$

For longitudinal polarization, the decay amplitudes of various diagrams and various effective operators are

$$\mathcal{M}_{enf}^{LL(N)} = \frac{32}{3}\pi C_F m_{B_c}^4 \int_0^1 d[x]\int_0^{1/\Lambda} b_1db_1b_2db_2\phi_{B_c}(x_1, b_1)\phi_T(x_2)\phi_D(x_3, b_1)\{[r_D(1 - x_3) - x_1 - x_2 + 1] \times E_{\rm enf}(t_a)h_{\rm enf}(x_1, (1 - x_2), x_3, b_1, b_2) + [r_D(1 - x_3) + x_1 - x_2 + x_3 - 1]E_{\rm enf}(t_b)h_{\rm enf}(x_1, x_2, x_3, b_1, b_2)\}, \tag{B1}$$

$$\begin{aligned}\mathcal{M}_{enf}^{LR(N)} = &-\frac{32}{3}\pi C_F r_T m_{B_c}^4 \int_0^1 d[x]\int_0^{1/\Lambda} b_1db_1b_2db_2\phi_{B_c}(x_1, b_1)\phi_D(x_3, b_1)\{[\phi_T^s(x_2)((r_D - 1)(x_1 + x_2) - r_Dx_3 + 1) \\ &+ \phi_T^t(x_2)(-x_1 - x_2 + r_D(x_1 + x_2 + x_3 - 2) + 1)] \cdot E_{\rm enf}(t_a)h_{enf}(x_1, (1 - x_2), x_3, b_1, b_2) \\ &+ [-\phi_T^s(x_2)(x_2 - x_1 + r_D(x_1 - x_2 - x_3 + 1)) + \phi_T^t(x_2)(x_2 - x_1 + r_D(x_1 - x_2 + x_3 - 1))] \\ &\cdot E_{\rm enf}(t_b)h_{enf}(x_1, x_2, x_3, b_1, b_2)\},\end{aligned} \tag{B2}$$

$$\mathcal{M}_{enf}^{SP(N)} = \frac{32}{3}\pi C_F m_{B_c}^4 \int_0^1 d[x]\int_0^{1/\Lambda} b_1db_1b_2db_2\phi_{B_c}(x_1, b_1)\phi_T(x_2)\phi_D(x_3, b_1)[(r_D(x_3 - 1) - x_1 - x_2 - x_3 + 2) \times E_{\rm enf}(t_a)h_{\rm enf}(x_1, (1 - x_2), x_3, b_1, b_2) + (r_D(x_3 - 1) + x_1 - x_2)E_{\rm enf}(t_b)h_{\rm enf}(x_1, x_2, x_3, b_1, b_2)], \tag{B3}$$

$$\mathcal{M}_{af}^{LL(N)} = 8\sqrt{\frac{2}{3}}C_F\pi f_{B_c}m_{B_c}^4 \int_0^1 dx_2dx_3 \int_0^{1/\Lambda} b_2db_2b_3db_3\phi_D(x_3, b_3)\{[2\phi_T^s(x_2)r_Dr_T(1 - x_3) - \phi_T(x_2)x_3] \times E_{af}(t_c)h_{af1}(x_2, x_3, b_2, b_3) + [\phi_T(x_2)x_2 + r_Tr_c(\phi_T^s(x_2) - \phi_T^t(x_2))]E_{af}(t_d)h_{af2}(x_2, x_3, b_2, b_3)\}, \tag{B4}$$

$$\mathcal{M}_{af}^{SP(N)} = -16\sqrt{\frac{2}{3}}C_Ff_{B_c}m_{B_c}^4\pi \int_0^1 dx_2dx_3 \int_0^{1/\Lambda} \phi_D(x_3, b_3)[(2\phi_T^s(x_2)r_T - r_D\phi_T(x_2)x_3)E_{af}(t_c)h_{af1}(x_2, x_3, b_2, b_3) + ((\phi_T^s(x_2) - \phi_T^t(x_2))r_Tx_2 + \phi_T(x_2)r_c) \cdot E_{af}(t_d)h_{af2}(x_2, x_3, b_2, b_3)], \tag{B5}$$

$$\begin{aligned}\mathcal{M}_{anf}^{LL(N)} = &-\frac{32}{3}C_F\pi m_{B_c}^4 \int_0^1 d[x]\int_0^{1/\Lambda} b_1db_1b_2db_2\phi_{B_c}(x_1, b_1)\phi_D(x_3, b_2)\{[\phi_T(x_2)(x_1 + x_2 - 1 + r_b) \\ &+ r_Tr_D(\phi_T^t(x_2)(x_1 + x_2 + x_3 - 2) + \phi_T^s(x_2)(x_1 + x_2 - x_3))]E_{anf}(t_e)h_{anf1}(x_1, x_2, x_3, b_1, b_2) \\ &+ [-\phi_T^s(x_2)r_Dr_T(x_1 - x_2 + x_3) + \phi_T^t(x_2)r_Dr_T(x_1 - x_2 - x_3) - \phi_T(x_2)(x_3 + r_c)] \\ &\times E_{anf}(t_f)h_{anf2}(x_1, x_2, x_3, b_1, b_2)\},\end{aligned} \tag{B6}$$

$$\mathcal{M}_{anf}^{LR(N)} = -\frac{32}{3} C_F \pi m_{B_c}^4 \int_0^1 d[x] \int_0^{1/\Lambda} b_1 db_1 b_2 db_2 \phi_{B_c}(x_1, b_1) \phi_D(x_3, b_2) \{[-(\phi_T^t(x_2) + \phi_T^s(x_2)) r_T (x_1 + x_2 - 1 - r_b) + \phi_T(x_2) r_D (x_3 - 1 - r_b)] \cdot E_{anf}(t_e) h_{anf1}(x_1, x_2, x_3, b_1, b_2) + [-(\phi_T^s(x_2) + \phi_T^t(x_2)) r_T (x_1 - x_2 + r_c) - \phi_T(x_2) r_D (x_3 - r_c)] \cdot E_{anf}(t_f) h_{anf2}(x_1, x_2, x_3, b_1, b_2)\}. \quad \text{(B7)}$$

For transverse polarization, the corresponding decay amplitudes are

$$\mathcal{M}_{enf}^{LL(s)} = -\frac{16}{\sqrt{3}} \pi C_F m_{B_c}^4 r_T \int_0^1 d[x] \int_0^{1/\Lambda} b_1 db_1 b_2 db_2 \phi_{B_c}(x_1, b_1) \phi_D^T(x_3, b_1) \{[(\phi_T^a(x_2) + \phi_T^v(x_2))(x_1 + x_2 - 1)] \times E_{\rm enf}(t_a) h_{enf}(x_1, (1 - x_2), x_3, b_1, b_2) + [\phi_T^a(x_2)(x_1 - x_2) + \phi_T^v(x_2)(-2(x_1 - x_2 + x_3 - 1) r_D + x_1 - x_2)] \cdot E_{enf}(t_b) h_{\rm enf}(x_1, x_2, x_3, b_1, b_2)\}, \quad \text{(B8)}$$

$$\mathcal{M}_{enf}^{LL(p)} = \mathcal{M}_{enf}^{LL(s)} |_{\phi_T^a \leftrightarrow \phi_T^v}, \quad \text{(B9)}$$

$$\mathcal{M}_{enf}^{LR(s)} = -\frac{16}{\sqrt{3}} \pi C_F m_{B_c}^4 \int_0^1 d[x] \int_0^{1/\Lambda} b_1 db_1 b_2 db_2 \phi_{B_c}(x_1, b_1) \phi_D^T(x_3, b_1) \phi_T^T(x_2) \{[r_D(r_D - 1)(x_3 - 1)] \times E_{\rm enf}(t_a) h_{\rm enf}(x_1, (1 - x_2), x_3, b_1, b_2) + [r_D(r_D - 1)(x_3 - 1)] E_{\rm enf}(t_b) h_{\rm enf}(x_1, x_2, x_3, b_1, b_2)\}, \quad \text{(B10)}$$

$$\mathcal{M}_{enf}^{LR(p)} = \mathcal{M}_{enf}^{LR(s)}, \quad \text{(B11)}$$

$$\mathcal{M}_{enf}^{SP(s)} = -\frac{16}{\sqrt{3}} \pi C_F m_{B_c}^4 r_T \int_0^1 d[x] \int_0^{1/\Lambda} b_1 db_1 b_2 db_2 \phi_{B_c}(x_1, b_1) \phi_D^T(x_3, b_1) \{[\phi_T^v(x_2)(2 r_D (x_1 + x_2 + x_3 - 2) - x_1 - x_2 + 1) + \phi_T^a(x_2)(x_1 + x_2 - 1)] E_{\rm enf}(t_a) h_{\rm enf}(x_1, (1 - x_2), x_3, b_1, b_2) + [(\phi_T^a(x_2) - \phi_T^v(x_2))(x_1 - x_2)] E_{enf}(t_b) h_{\rm enf}(x_1, x_2, x_3, b_1, b_2)\}, \quad \text{(B12)}$$

$$\mathcal{M}_{enf}^{SP(p)} = -\mathcal{M}_{enf}^{SP(s)} |_{\phi_T^a \leftrightarrow \phi_T^v}, \quad \text{(B13)}$$

$$\mathcal{M}_{af}^{LL(s)} = 4\sqrt{2} C_F \pi f_{B_c} r_D m_{B_c}^4 \int_0^1 dx_2 dx_3 \int_0^{1/\Lambda} b_2 db_2 b_3 db_3 \phi_D^T(x_3, b_3) \{[-r_T(\phi_T^a(x_2)(1 - x_3) + \phi_T^v(x_2)(1 + x_3))] \times E_{af}(t_c) h_{af1}(x_2, x_3, b_2, b_3) + [r_T(\phi_T^a(x_2)(x_2 - 1) + \phi_T^v(x_2)(x_2 + 1)) - \phi_T^T(x_2) r_c] E_{af}(t_d) h_{af2}(x_2, x_3, b_2, b_3)\}, \quad \text{(B14)}$$

$$\mathcal{M}_{af}^{LL(p)} = \mathcal{M}_{af}^{LL(s)} |_{\phi_T^a \leftrightarrow \phi_T^v}, \quad \text{(B15)}$$

$$\mathcal{M}_{af}^{SP(s)} = 8\sqrt{2} C_F \pi f_{B_c} m_{B_c}^4 \int_0^1 dx_2 dx_3 \int_0^{1/\Lambda} b_2 db_2 b_3 db_3 \phi_D^T(x_3, b_3) \{[r_T(\phi_T^a(x_2) + \phi_T^v(x_2))] E_{af}(t_c) h_{af1}(x_2, x_3, b_2, b_3) - [r_D(\phi_T^T(x_2)(r_D^2 - 1) + 2\phi_T^v(x_2) r_T r_c)] E_{af}(t_d) h_{af2}(x_2, x_3, b_2, b_3)\}, \quad \text{(B16)}$$

$$\mathcal{M}_{af}^{SP(p)} = \mathcal{M}_{af}^{SP(s)} |_{\phi_T^a \leftrightarrow \phi_T^v}, \quad \text{(B17)}$$

$$\mathcal{M}_{anf}^{LL(s)} = \frac{16}{\sqrt{3}} C_F \pi r_D m_{B_c}^4 \int_0^1 d[x] \int_0^{1/\Lambda} b_1 db_1 b_2 db_2 \phi_{B_c}(x_1, b_1) \phi_D^T(x_3, b_2) \{[-\phi_T^T(x_2) r_D (x_3 - 1) - 2\phi_T^v(x_2) r_T r_b] \times E_{anf}(t_e) h_{anf1}(x_1, x_2, x_3, b_1, b_2) + [\phi_T^T(x_2) r_D x_3 + 2\phi_T^v(x_2) r_T r_c] E_{anf}(t_f) h_{anf2}(x_1, x_2, x_3, b_1, b_2)\}, \quad \text{(B18)}$$

$$\mathcal{M}_{anf}^{LL(p)} = \mathcal{M}_{anf}^{LL(s)} |_{\phi_T^v \to \phi_T^a}, \quad \text{(B19)}$$

$$\mathcal{M}_{anf}^{LR(s)} = \frac{16}{\sqrt{3}} C_F \pi m_{B_c}^4 \int_0^1 d[x] \int_0^{1/\Lambda} b_1 db_1 b_2 db_2 \phi_{B_c}(x_1, b_1) \phi_D^T(x_3, b_2) \{[-(\phi_T^a(x_2) + \phi_T^v(x_2)) r_T (x_1 + x_2 - 1 - r_b) + \phi_T^T(x_2) r_D (x_3 - 1 - r_b)] E_{anf}(t_e) h_{anf1}(x_1, x_2, x_3, b_1, b_2) - [r_T(\phi_T^a(x_2) + \phi_T^v(x_2))(x_1 - x_2 + r_c) + \phi_T^T(x_2) r_D (x_3 - r_c)] E_{anf}(t_f) h_{anf2}(x_1, x_2, x_3, b_1, b_2)\}, \tag{B20}$$

$$\mathcal{M}_{anf}^{LR(p)} = \mathcal{M}_{anf}^{LR(s)}. \tag{B21}$$

[1] F. Abe *et al.* (CDF Collaboration), Phys. Rev. Lett. **81**, 2432 (1998); Phys. Rev. D **58**, 112004 (1998).
[2] T. Aaltonen *et al.* (CDF Collaboration), Phys. Rev. Lett. **100**, 182002 (2008); V.M. Abazov *et al.* (D0 Collaboration), Phys. Rev. Lett. **101**, 012001 (2008).
[3] N. Brambilla *et al.* (Quarkonium Working Group), Report No. CERN-2005-005.
[4] N. Brambilla *et al.*, Eur. Phys. J. C **71**, 1534 (2011).
[5] I.I. Bigi, Phys. Lett. B **371**, 105 (1996).
[6] M. Beneke and G. Buchalla, Phys. Rev. D **53**, 4991 (1996).
[7] C.H. Chang and Y.Q. Chen, Phys. Rev. D **49**, 3399 (1994).
[8] C. H. Chang, Y. Q. Chen, and R. J. Oakes, Phys. Rev. D **54**, 4344 (1996).
[9] M. Lusignoli, M. Masetti, and S. Petrarca, Phys. Lett. B **266**, 142 (1991).
[10] N. Brambilla and A. Vairo, Phys. Rev. D **62**, 094019 (2000).
[11] N. Brambilla, A. Pineda, J. Soto, and A. Vairo, Rev. Mod. Phys. **77**, 1423 (2005).
[12] V. V. Kiselev, A. E. Kovalsky, and A. K. Likhoded, Nucl. Phys. **B585**, 353 (2000).
[13] V. V. Kiselev, J. Phys. G **30**, 1445 (2004).
[14] S. Descotes-Genon, J. He, E. Kou, and P. Robbe, Phys. Rev. D **80**, 114031 (2009).
[15] N. Sharma, Phys. Rev. D **81**, 014027 (2010).
[16] N. Sharma and R.C. Verma, Phys. Rev. D **82**, 094014 (2010).
[17] G López Castro, H. B. Mayorga, and J. H. Muñoz, J. Phys. G **28**, 2241 (2002).
[18] J.F. Sun, G.F. Xue, Y.L. Yang, G.R. Lu, and D.S. Du, Phys. Rev. D **77**, 074013 (2008); **77**, 114004 (2008); Eur. Phys. J. C **60**, 107 (2009).
[19] Y.L. Yang, J.F. Sun, and N. Wang, Phys. Rev. D **81**, 074012 (2010).
[20] J. F. Cheng, D. S. Du, and C. D. Lü, Eur. Phys. J. C **45**, 711 (2006).
[21] X. Liu, Z. J. Xiao, and C. D. Lü, Phys. Rev. D **81**, 014022 (2010).
[22] X. Liu and Z.J. Xiao, Phys. Rev. D **82**, 054029 (2010).
[23] X. Liu and Z. J. Xiao, Phys. Rev. D **81**, 074017 (2010).
[24] X. Liu and Z. J. Xiao, J. Phys. G **38**, 035009 (2011).
[25] Z. J. Xiao and X. Liu, Phys. Rev. D **84**, 074033 (2011); Z. Rui, Z. T. Zou, and C. D. Lü, Phys. Rev. D **86**, 074019 (2012).
[26] Z. Rui, Z. T. Zou, and C. D. Lü, Phys. Rev. D **86**, 074008 (2012).
[27] W. Wang, Phys. Rev. D **83**, 014008 (2011).
[28] H. Y. Cheng, Y. Koike, and K. C. Yang, Phys. Rev. D **82**, 054019 (2010).
[29] H.-Y. Cheng and K.-C. Yang, Phys. Rev. D **83**, 034001 (2011).
[30] A. C. Katoch and R. C. Verma, Phys. Rev. D **49**, 1645 (1994); **52**, 1717 (1995); **55**, 7315(E) (1997).
[31] G. López Castro and J. H. Muñoz, Phys. Rev. D **55**, 5581 (1997).
[32] J. H. Muñoz, A. A. Rojas, and G. López Castro, Phys. Rev. D **59**, 077504 (1999).
[33] C. S. Kim, B. H. Lim, and S. Oh, Eur. Phys. J. C **22**, 683 (2002).
[34] C. S. Kim, B. H. Lim, and S. Oh, Eur. Phys. J. C **22**, 695 (2002); **24**, 665(E) (2002).
[35] C. S. Kim, B. H. Lim, and S. Oh, Phys. Rev. D **67**, 014002 (2003).
[36] J.H. Muňoz and N. Quintero, J. Phys. G **36**, 095004 (2009).
[37] N. Sharma, R. Dhir, and R.C. Verma, Phys. Rev. D **83**, 014007 (2011).
[38] C. S. Kim, B. H. Lim, and S. Oh, Phys. Rev. D **67**, 014011 (2003).
[39] W. Wang, Phys. Rev. D **85**, 051301 (2012).
[40] Z. T. Zou, X. Yu, and C. D. Lü, Phys. Rev. D **86**, 094001 (2012); **86**, 094015 (2012); Z.T. Zou, Z. Rui, and C. D. Lü, arXiv:1204.3144.
[41] C.-D. Lü and K. Ukai, Eur. Phys. J. C **28**, 305 (2003).
[42] Y. Li and C. D. Lu, J. Phys. G **29**, 2115 (2003); High Energy Phys. Nucl. Phys. **27**, 1062 (2003).
[43] Y. Li, C. D. Lü, Z. J. Xiao, and X. Q. Yu, Phys. Rev. D **70**, 034009 (2004).
[44] A. Ali, G. Kramer, Y. Li, C.-D. Lü, Y.-L. Shen, W. Wang, and Y.-M. Wang , Phys. Rev. D **76**, 074018 (2007).
[45] C. D. Lü and K. Ukai, Eur. Phys. J. C **28**, 305 (2003).
[46] R. H. Li, C. D. Lu, and H. Zou, Phys. Rev. D **78**, 014018 (2008).
[47] M.J. Morello *et al.* (CDF Collaboration), CDF public note, Report No. 10498, 2011.
[48] K. Nakamura *et al.* (Particle Data Group), J. Phys. G **37**, 075021 (2010).
[49] Y. Y. Keum, H.-n. Li, and A. I. Sanda, Phys. Lett. B **504**, 6 (2001); Phys. Rev. D **63**, 054008 (2001).
[50] C. D. Lü, K. Ukai, and M. Z. Yang, Phys. Rev. D **63**, 074009 (2001).

[51] H.-n. Li, Prog. Part. Nucl. Phys. **51**, 85 (2003), and references therein.
[52] H. n. Li, Phys. Rev. D **52**, 3958 (1995); C. Y. Wu, T. W. Yeh, and H. n. Li, Phys. Rev. D **53**, 4982 (1996); Y. Y. Keum, T. Kurimoto, H.-n. Li, C.-D. Lü, and A. I. Sanda, Phys. Rev. D **69**, 094018 (2004); C. D. Lü, Phys. Rev. D **68**, 097502 (2003).
[53] C. D. Lü, Eur. Phys. J. C **24**, 121 (2002); J. F. Cheng, D. S. Du, and C. D. Lü, Eur. Phys. J. C **45**, 711 (2006).
[54] C. W. Bauer, D. Pirjol, I. Z. Rothstein, and I. W. Stewart, Phys. Rev. D **70**, 054015 (2004).
[55] G. Buchalla, A. J. Buras, and M. E. Lautenbacher, Rev. Mod. Phys. **68**, 1125 (1996).
[56] A. Ali, G.kramer, and C. D. Lü, Phys. Rev. D **58**, 094009 (1998).
[57] H. N. Li, Phys. Rev. D **66**, 094010 (2002).
[58] H. N. Li and B. Tseng, Phys. Rev. D **57**, 443 (1998).
[59] C. D. Lü and M. Z. Yang, Eur. Phys. J. C **23**, 275 (2002).
[60] T. Kurimoto, H. n. Li, and A. I. Sanda, Phys. Rev. D **67**, 054028 (2003).
[61] R. H. Li, C. D. Lu, and H. Zou, Phys. Rev. D **78**, 014018 (2008).
[62] H. Zou, R. H. Li, X. X. Wang, and C. D. Lu, J. Phys. G **37**, 015002 (2010).
[63] R. H. Li, C. D. Lu, A. I. Sanda, and X. X. Wang, Phys. Rev. D **81**, 034006 (2010).
[64] E. Follana, C. T. H. Davies, G. P. Lepage, and J. Shigemitsu (HPQCD Collaboration and UKQCD Collaboration), Phys. Rev. Lett. **100**, 062002(2008).
[65] A. V. Manohar and M. B. Wise, Cambridge Monogr. Part. Phys., Nucl. Phys., Cosmol. **10**, 1 (2000).
[66] T. M. Aliev and M. A. Shifman, Phys. Lett. **112B**, 401 (1982); Yad. Fiz. **36**, 1532 (1982) [Sov. J. Nucl. Phys. **36**, 891 (1982)].
[67] T. M. Aliev, K. Azizi, and V. Bashiry, J. Phys. G **37**, 025001 (2010).
[68] H.-Y. Cheng and R. Shrock, Phys. Rev. D **84**, 094008 (2011).
[69] D. M. Li, H. Yu, and Q. X. Shen, J. Phys. G **27**, 807 (2001).
[70] Y. N. Gao, J. B. He, P. Robbe, M.-H. Schune, and Z. W. Yang, Chin. Phys. Lett. **27**, 061302 (2010).
[71] A. V. Gritsan, *Proceedings of the Flavor Physics and CP Violation Conference, Bled, 2007*, eConf. C070512 (2007).
[72] J. G. Körner and G. R. Goldstein, Phys. Lett. **89B**, 105 (1979).
[73] A. L. Kagan, Phys. Lett. B **601**, 151 (2004).
[74] H.-n. Li and K. Ukai, Phys. Lett. B **555**, 197 (2003).